表　NMDA受容体グリシン調節部位作動薬の統合失調症に対する臨床試験

報告者	発表年	物質名	内服量	期間（週間）	患者数（人）	方法	併用：抗精神病薬	陽性症状	陰性症状	認知機能	文献番号
Tsai et al.	1998	D-Serine	30mg/kg/日	6	31	double-blind	多種（clozapineなし）	改善	改善	改善	49
Tsai et al.	1999	D-Serine	30mg/kg/日	6	20	double-blind	Clozapine	不変	不変	不変	50
Heresco-Levy et al.	2005	D-Serine	30mg/kg/日	6	39	double-blind, crossover	Risperidone or Olanzapine	改善	改善	改善	22
Javitt et al.	1994	Glycine	0.4g/kg/日(=30g/日)	8	14	double-blind	多種		改善		25
Heresco-Levy et al.	1996	Glycine	0.8g/kg/日(=60g/日)	6	11	double-blind, crossover	多種		改善	改善	17
Heresco-Levy et al.	1999	Glycine	0.8g/kg/日(=60g/日)	6	22	double-blind, crossover	多種（clozapine含む）		改善		18
Potkin et al.	1999	Glycine	30g/日	12	19	double-blind	Clozapine	不変～悪化	不変		43
Evins et al.	2000	Glycine	60g/日	8	27	double-blind	Clozapine	不変	不変	不変	8
Javitt et al.	2001	Glycine			21		Clozapine or Olanzapine		改善		27
Heresco-Levy et al.	2004	Glycine	0.8g/kg/日(=60g/日)	6	17	double-blind, crossover	Risperidone or Olanzapine	改善	改善	改善	21
Diaz et al.	2005	Glycine	60g/日	12	12	double-blind, crossover	Clozapine	不変	不変		5
Cascella et al.	1994	D-cycloserine	250mg/日	6		open-label study	多種	悪化			3
Goff et al.	1995	D-cycloserine	50mg/日	2	9	single blind, rater blind	多種		改善		10
Rosse et al.	1996	D-cycloserine	10/30mg/日	4	13	double-blind	Molindone	不変	不変		44
Goff et al.	1996	D-cycloserine	50mg/日	2	10	single blind, rater blind	Clozapine		悪化		11
Heresco-Levy et al.	1998	D-cycloserine	50mg/日	6	9	double-blind	多種（clozapine含む）		改善		18
Goff et al.	1999a	D-cycloserine	50mg/日	8	47	double-blind	多種（clozapineなし）		改善	改善	12
Goff et al.	1999b	D-cycloserine	50mg/日	6	17	double-blind, crossover	Clozapine		悪化		13
van Berckel et al.	1999	D-cycloserine	100mg/日	8	26	double-blind	多種（clozapineなし）	悪化	悪化		55
Evins et al.	2002	D-cycloserine	50mg/日	2	10	single-blind	risperidone		改善		9
Heresco-Levy et al.	2002	D-cycloserine	50mg/日	6	24	double-blind, crossover	多種（clozapineなし）		改善		20
Duncan et al.	2004	D-cycloserine	50mg/日	4	22	double-blind	多種（clozapineなし）		不変	不変	6
Goff et al.	2005	D-cycloserine	50mg/日	24	26	double-blind	多種（clozapineなし）		不変	不変	14
Tsai et al.	2006	D-Alanine	100mg/kg/日	6	32	double-blind	多種（clozapineなし）	改善	改善	改善	51
Tsai et al.	2004	Sarcosine	2g/日	6	38	double-blind	多種(clozapineなし)	改善	改善	改善	52
Lane et al.	2005	Sarcosine or D-Serine	2g/日	6	65	double-blind	多種(clozapineなし)	改善	改善	改善	33
Lane et al.	2006	Sarcosine	2g/日	6	20	double-blind	Clozapine	不変	不変	不変	34

※ Sarcosineの方が改善効果は大きい

討されている。

1. 動物モデルにおける検討

PCPをはじめとするNMDA受容体遮断薬が動物に発現させる異常行動は，統合失調症状のモデルと考えられる。例えばラットでは，PCP投与により，移所運動量の亢進，常同行動の出現などの異常が出現する。既存の抗精神病薬は，これらの変化を部分的にしか抑制することができない[47]。しかし，D-セリン，D-アラニン，グリシンなどのNMDA受容体コ・アゴニストは，PCP誘発性の異常行動を全体的に抑制する[48]。D-アミノ酸の抑制効果は，グリシン結合部位への親和性に一致した立体特異性(D-セリン＞L-セリン，D-アラニン＞L-アラニン)を示すことや，この部位の選択的拮抗薬の前処置によって減弱すること[48]から，NMDA受容体グリシン結合部位の刺激を介してもたらされたと考えられる。また，グリシンは，PCP慢性投与動物の前頭葉におけるamphetamine単回投与によるDA遊離の増大を抑制する[28]。さらに，PCP急性投与後にみられる前頭葉内のDA伝達亢進は，D-アラニンによって立体特異的に抑制される。

以上の結果は，グリシン結合部位の刺激が，統合失調症の陽性症状だけでなく陰性症状にも効果を示すことを示唆している。

2. 臨床試験(表)

これまで実際に臨床試験が行われたグリシン結合部位作動薬は，以下のようなものがある。

1) グリシン

グリシンによる統合失調症治療の試みは，1988年にWaziriにより初めて報告された[57]。抗精神病薬との併用により陰性症状が改善されたという報告が多く，メタ解析でも有効性が確認された[53]。ただし，clozapineとの併用では，clozapine単独の効果と有意差がない。グリシンは，他の中性アミノ酸と同様に脳内移行性が低いため，高用量(60g/日)を用いなければならず，経口摂取の負担が大きい。また，腎臓におけるアンモニアの発生，抑制性グリシン受容体への作用などの問題に留意する必要がある[26,29,58,59]。

2) D-サイクロセリン

D-サイクロセリンは，細胞壁ペプチドグリカン生合成阻害作用を持ち，抗結核薬として長く使用されてきたため，安全性に関する臨床データは豊富である[23]。中枢神経系においては，NMDA受容体グリシン結合部位に対して部分作動薬として働く[23]。そのため，投与量によって作動薬として作用する場合と拮抗薬として作用する場合が起こりうる。したがって，脳への移行性が比較的高いことは利点であるが，治療用量の設定が難しい。1994年以降，統合失調症治療に応用され，高用量(250 mg/日)では精神症状が悪化した[3]が，50 mg/日を定型または非定型(risperidone, olanzapine)抗精神病薬と併用投与した場合は，陰性症状の改善が認められたという報告が多い[7,10,12,18,20]。Clozapineとの併用ではむしろ悪化したという[11,13]。ただし，最近の長期間の投与試験では，D-サイクロセリンはfull agonistに比べて治療効果は低く，陰性症状や認知機能に関して有意な治療効果がみられなかった[14]。

3) D-セリン

1998年にTsaiら[49]は，定型抗精神病薬で治療中の症状の変動が少ない慢性期統合失調症患者に対して，D-セリン(2 g/日)を併用経口投与し，定型抗精神病薬抵抗性の陰性症状，認知機能障害および陽性症状の改善効果を認めたと報告した。その後，非定型抗精神病薬との併用でも同様の改善効果が確認された[18]が，clozapineとの併用ではclozapine単独との差異は認められなかった[50]。D-セリンは，グリシン結合部位の選択的full agonistであり臨床効果も高いが，グリシンと同様に脳への移行性が低いために高用量を必要とし，腎毒性(尿細管壊死)を持つ可能性を否定できない点などが問題である[59]。

4) D-アラニン

D-セリンと同じく，NMDA受容体グリシン結合部位の選択的full agonistであるD-アラニ

ン(7 g/日)も，抗精神病薬と併用投与した統合失調症患者において，陽性症状，陰性症状，認知機能障害などのスコアを改善することが報告された[51]。D-アラニンにも脳への移行を図るのに高用量を要する欠点がある。

5) グリシントランスポーター阻害薬

グリシンの投与量が著しく高い点を克服するために，血液脳関門を透過しやすく，シナプス間隙のグリシン濃度上昇作用が期待できるグリシントランスポーター阻害薬の開発が試みられている。現在，NMDA受容体のように前脳部に多く存在するⅠ型グリシントランスポーターを阻害するN-methyl-glycine (sarcosine)，glycyldodecylamide(GDA)，N[3-(4'-fluorophenyl)-3-(4'-henyl-phenoxy) propyl]-sarcosine (NEPS)，Org24598などが開発中であるが，臨床試験が行われているのはsarcosineのみである[52]。Tsaiらの研究[33]によると，慢性統合失調症患者の急性増悪に対する改善効果は，グリシンやD-セリンに比較して高い。ただし，最近の報告[34]では，clozapineとの併用では差異がみられなかったという。

5 内在性D-セリンと統合失調症

D-セリンは，脳を中心にヒトを含む哺乳類の組織に一生の間高い濃度を保つ例外的なD-アミノ酸である。成熟期には脳選択的に高い濃度で存在し，脳内濃度は前脳部に高く後脳では痕跡程度になる不均一な分布を示す[41]。この脳内分布と発達に伴う変化は，NMDA受容体R2Bサブユニットと酷似しており，D-セリンは，前脳部における内在性のNMDA受容体コ・アゴニストであると推測されている[41]。したがって，統合失調症では，D-セリンのシグナル減少のためにNMDA受容体機能が低下している可能性が注目されている[41]。

D-セリンは，脳内のNMDA受容体が生理的に機能するために，一定の細胞外濃度が維持される必要があると考えられ[39]，その異常な減少が統合失調症で推測されるNMDA受容体機能の低下の原因である可能性がある。これまでの研究では，統合失調症患者の死後脳各部位におけるD-セリン濃度の低下は見いだされていない[41]。一方，D-セリンシグナルを受けるグリシン結合部位が種々の脳部位で増加しているという報告[24]があり，統合失調症では何らかの機序で細胞外D-セリンの減少が生じ，代償的にグリシン結合部位が増加している可能性がある。また，血液中や脳脊髄液中のL-セリンに対するD-セリンの比が統合失調症患者で減少しているという報告[15,16]もあり，統合失調症におけるD-セリンの代謝および機能の分子機構についての解明が待たれる。

これらの分子は，NMDA受容体グリシン結合部位に対するD-セリンシグナルを調節する，統合失調症治療薬の標的としても重要である。例えば，D-セリンに特異的なトランスポーターが同定されれば，その阻害薬が優れた抗精神病薬になる可能性がある。

6 おわりに

統合失調症の薬物療法が始まって半世紀が過ぎた。その間に，多くの抗精神病薬が開発され臨床に応用されてきた。これまでの治療薬開発は，chlorpromazine，haloperidol，clozapineといった臨床効果が認められた特定の薬剤をモデルとして行われてきたため，モデルとなっている薬剤の治療効果を大きく上回る治療薬の開発は困難であった。治療抵抗性症状への対策として，NMDA受容体機能促進薬以外にも，選択的セロトニン取り込み阻害薬(SSRI)，エストロゲン，あるいはアセチルコリンエステラーゼ阻害薬，などが試みられている[7]。また，clozapineのDA伝達系以外への直接的な薬理作用に着目し，選択的α2受容体遮断薬idazoxanを抗精神病薬と併用したところ，抗精神病薬単独投与に比較して症状評価尺度の改善度が有意に高かったという[37]。しかし，clozapineも含め，これま

でのところ陰性症状や認知機能に顕著な効果が認められた向精神薬はない。

本稿で紹介したNMDA受容体－D-セリンシグナル系を標的とする治療法は，既存の向精神薬にはない薬理作用を導入する点で期待されるが，難治性症状のモデル化が難しいことや，脳内移行，標的部位への親和性などの，克服すべき問題を多く抱えている。今後，NMDA受容体－D-セリンシステムの分子機構や関連するゲノム領域における調節メカニズムに関する研究がさらに発展し，NMDA受容体－D-セリンシグナルカスケードへの選択的で強力な作用を持ち，脳内移行性と安全性に優れた新規治療薬の開発が促進されることが望まれる。

文献

1) Anis NA, Berry SC, Burton R et al : The dissociative anaesthetics, ketamine and phencyclidine selectively reduce excitation of central mammalian neurons by N-methyl-aspartate. Br J Pharmacol 79 : 565–575, 1983
2) Buchanan RW, Carpenter WT : Schizophrenia. In Sadock BJ, Sadock VA (Eds): Kaplan & Sadock's Comprehensive Textbook of Psychiatry, 8th edition Volume 1. Lippinott Williams & Wilkins,Philadelphia, pp1329–1558, 2005
3) Cascella NG, Macciardi F, Cavallini C et al : D-cycloserine adjuvant therapy to conventional neurolepyic treatment in schizophrenia: an open-label study. J Neural Transm Gen Sect 95 :105, 1994
4) Dannysz W, Parsons AC : Glycine and N-methyl-D-aspartate receptors: physiological significance and possible therapeutic applications. Pharmacol Rev 50 : 597–664, 1998
5) Diaz P, Bhaskara S, Dursun SM et al : Double-blind, placebo-controlled, crossover trial of clozapine plus glycine in refractory schizophrenia negative results. J Clin Psychopharmacol 25 : 277–278, 2005
6) Duncan EJ, Szilagyi S, Schwartz MP et al : Effects of D-cycloserine on negative symptoms in schizophrenia. Schizophr Res 71 : 239–248, 2004
7) Erhart SM, Marder SR, Carpenter WT : Treatment of schizophrenia negative symptoms: future prospects. Schizophr Bull 32 : 234–237, 2006
8) Evins AE, Fitzgerald SM, Wine L et al : Placebo-controlled trial of glycine added to clozapine in schizophrenia. Am J Psychiatry 157 : 826–828, 2000
9) Evins AE, Amico E, Goff DC et al : D-Cycloserine added to risperidone in patients with primary negative symptoms of schizophrenia. Schizophrenia Research 56 : 19–23, 2002
10) Goff DC, Tsai G, Coyle JT et al : Dose-finding trial of D-cycloserine added to neuroleptics for negative symptoms in schizophrenia. Am J Psychiatry 152 : 1213–1215, 1995
11) Goff DC, Tsai G, Coyle JT et al : D-Cycloserine added to clozapine for patients with schizophrenia. Am J Psychizatry 153 : 1628–1630, 1996
12) Goff DC, Tsai G, Coyle JT et al : A placebo-controlled trial of D-cycloserine added to conventional neuroleptics in patients with schizophrenia. Arch Gen Psyhiatry 56 : 21–27, 1999
13) Goff DC, Henderson DC, Amico E et al : A placebo-controlled crossover trial of D-cycloserine added to clozapine in patients with schizophrenia. Biol Psychiatry 45 : 512–514, 1999
14) Goff DC, Herz L, Schoenfeld D et al : A six-month, placebo-controlled trial of D-cycloserine co-administered with conventional antipsychotics in schizophrenia patients. Psychopharmacology 179 : 144–150, 2005
15) Hashimoto K, Fukushima T, Iyo M et al : Decreased serum levels of D-serine in patients with schizophrenia: evidence in support of the N-methyl-D-aspartate receptor hypofunction hypothesis of schizophrenia. Arch Gen Psychiatry 60 : 572–576, 2003
16) Hashimoto K, Engberg G, Iyo M et al : Reduced D-serine to total serine ratio in the cerebrospinal fluid of drug naïve schizophrenic patients. Prog Neuropsychopharmacol Biol Psychiatry 29 : 767–769, 2005
17) Heresco-Levy U, Javitt DC, Ermilov M et al : Double-blind, placebo-controlled, crossover trial of glycine adjuvant therapy for treatment-resistant schizophrenia. Br J Psychiatry 169 : 610–617, 1996
18) Hersco-Levy U, Javitt DC, Shimoni J et al : Double-blind, placebo-controlled, crossover trial of D-cycloserine adjuvant therapy for trentment-resistant schizophrenia. Int J Neuropsychopharmacol 1 : 131–135, 1998
19) Heresco-Levy U, Javitt DC, Ermilov M et al :

Efficacy of high-dose glycine in the treatment of enduring negative symptoms of schizophrenia. Arch Gen Psychiatry 56 : 29–36, 1999
20) Hersco-Levy U, Ermilov M, Javitt DC et al : Placebo-controlled trial of D-cycloserine added to conventional neuroleptics, olanzapine, or risperidone in schizophrenia. Am J Psychiatry 159 : 480–482, 2002
21) Heresco-Levy U, Ermilov M, Lichtenberg P et al : High-dose glycine added to olanzapine and risperidone for the treatment of schizophrenia. Biol Psychiatry 55 : 165–171, 2004
22) Heresco-Levy U, Javitt DC, Ermilov M et al : D-Serine efficacy as add-on pharmacotherapy to risperidone and olanzapine for treatment-refractory schizophrenia. Biol Psychiatry 57 : 577–585, 2005
23) Hood WF, Compton RP, Monahan JB : D-Cycloserine: a ligand for the N-methyl-D-aspartate coupled glycine receptor has partial agonist characteristics. Neurosci Lett 98 : 91–91, 1989
24) Ishimaru M, Kurumaji A, Toru M : Increases in strychnine-insensitive glycine binding sites in cerebral cortex of chronic schizophrenics: evidence for glutamate hypothesis. Biol Psychiatry 35 : 84–95, 1994
25) Javitt DC, Zylberman I, Zukin SR et al : Amelioration of negative symptoms in schizophrenia by glycine. Am J Psychiatry 151 : 1234–1236, 1994
26) Javitt D : Correspondence; Glycine therapy of schizophrenia. Biol Psychiatry 40 : 684–685, 1996
27) Javitt DC, Silipo G, Cienfuegos A et al : Adjunctive high-dose glycine in the treatment of schizophrenia. Int J Neuropsychopharmacol 4 : 385–391, 2001
28) Javitt DC, Balla A, Sershen H et al : Reversal of phencyclidine-induced dopaminergic dysregulation by N-methyl-D-aspartate receptor/glycine site-agonists. Neuropsychopharmacology 29 : 300–307, 2004
29) Javitt DC : Glutamate as a therapeutic target in psychiatric disorders. Mol Psychiatry 9 : 984–997
30) Jentsch JD, Roth RH : The neuropsychopharmacology of phencyclidine: from NMDA receptor hypofunction to the dopamine hypothesis of schizophrenia. Neuropsychopharmacology 20 : 201–225, 1999
31) Kapur S, Seeman P : Does fast dissociation from the dopamine D_2 receptor explain the action of atypical antipsychotics? A new hypothesis. Am J Psychiatry 158 : 360, 2001
32) Krystal JH, Karper LP, Charney DS et al : Subanesthetic effects of the noncompetitive NMDA antagonist, ketamine, in humans: psychotomimetic, perceptual, cognitive, and neuroendocrine responses. Arch Gen Psychiatry 51 : 199–214, 1994
33) Lane HY, Chang YC, Tsai GE et al : Sarcosine or D-serine add-on treatment for acute exacerbation of schizophrenia: a randomized, double-blind, placebo- controlled study. Arch Gen Psychiatry 62 : 1196–1204, 2005
34) Lane HY, Huang CL, Wu PL et al : Glycine transporter I inhibitor, N-methylglycine (sarcosine), added to clozapine for the treatment of schizophrenia. Biol Psychiatry 60 : 645–649, 2006
35) Laruelle M, Frankle WG, Abi-Daragham A et al : Mechanism of action of antipsychotic drugs: from dopamine D2 receptor antagonism to glutamate NMDA facilitation. Clin Ther 27 [Suppl A]: S16–S24, 2005
36) Lieberman JA, Kane JM, Alvir J : Provocative tests with psychostimulant drugs in schizophrenia. Psychopharmacology 91 : 315–433, 1987
37) Lindstrom LH : Schizophrenia, the dopamine hypothesis and alpha2-adrenoceptor antagonists. Trends Pharmacol Sci 21 : 198–199, 2000
38) Meltzer HY, Matsubara S, Lee J-C : Classification of typical and atypical antipsychotic drugs on the basis of dopamine D-1, D-2 and serotonin2 pKi values. J Pharmacol Exp Ther 251 : 238,.1989
39) 西川 徹：脳内 D-セリンの代謝と生理作用．細胞工学 23 : 1180–1185, 2004
40) 西川 徹：統合失調症のグルタミン酸仮説．生体の科学 55 : 544–545, 2004
41) 西川 徹：ヒトの脳に存在する遊離型 D-セリンの機能と病態．精神神経疾患の治療への応用．ファルマシア 41 : 863–868, 2005
42) Petersen RC, Stillman RC : Phencyclidine: An overview. In Peterson RC, Stillman RC (Eds): Phencyclidine (PCP) abuse: An appraisal. NIDA research monograph 21, U. S. government printing office, Washington DC, pp1–17, 1978
43) Potkin SG, Jin Y, Bunney BG, Costa J et al : Effect of clozapine and adjunctive high-dose glycine in treatment-resistant schizophrenia. Am J Psychiatry 156 : 145–147, 1999
44) Rosse RB, Fay-McCarthy M, Kendrick K et al : D-cycloserine adjuvant therapy to molindone in the

treatment of schizophrenia. Clin Neuropharmacol 19 : 444–450, 1996
45) Seeman P, Lee T, Chan-wong M et al : Antipsychotic drug doses and neuroleptic/dopamine receptors. Nature 261 : 717–719, 1976
46) Shirayama Y, Mitsushio H, Takahashi K et al : Differential effects of haloperidol on phencyclidine-induced reduction in substance P contents in rat brain regions. Synapse 35 : 292–299, 2000
47) Tanii Y, Nishikawa T, Hashimoto A et al : Stereoselective inhibition by D- and L-alanine of phencyclidine-induced locomotor stimulation in the rat. Brain Res 563 : 281–284, 1991
48) Tanii Y, Nishikawa T, Hashimoto A et al : Stereoselective antagonism by enantiomers of alanine and serine of phencyclidine-induced hyperactivity, stereotypy and ataxia in the rat. J Pharmacol Exp Ther 269 : 1040–1048, 1994
49) Tsai G, Yang P, Coyle JT et al : D-Serine added to antipsychotics for the treatment of schizophrenia. Biol Psychiatry 44 : 1081–1089, 1998
50) Tsai GE, Yang P, Coyle JT et al : D-Serine added to clozapine for the treatment of schizophrenia. Am J Psychiatry 156 : 1822–1825, 1999
51) Tsai GE, Yang P, Chong MY et al : D-Alanine added to antipsychotics for the treatment of schizophrenia. Biol Psychiatry 59 : 230–234, 2006
52) Tsai GE, Lane HY, Lange N et al : Glycine transporter I inhibitor, N-Methylglycine (Sarcosine), added to antipsychotics for the treatment of schizophrenia. Biol Psychiatry 55 : 452–456, 2004
53) Tuominen HJ, Tiihonen J, Wahlbeck K : Glutamatergic drugs for schizophrenia: a systematic review and meta-analysis. Schizophrenia Research 72 : 225–234, 2005
54) Umino A, Takahashi K, Nishikawa T : Characterization of the phencyclidine-induced increase in prefrontal cortical dopamine metabolism in the rat. Br J Pharmacol 124 : 377–385, 1998
55) van Berckel BN, Evenblij CN, van Loon BJ et al : D-cycloserine increases positive symptoms in chronic schizophrenic patients when administered in addition to antipsychotics: a double-blind, parallel, placebo-controlled study. Neuropsychopharmacology 21 : 203–210, 1999
56) Vollenweider FX, Leenders KL, Angst J et al : Differential psychopathology and patterns of cerebral glucose utilization produced by (S)- and (R)-ketamine in healthy volunteers using positron emission tomography (PET). Eur Neuropsychopharmacol 7 : 25–38, 1997
57) Waziri R : Glycine therapy of schizophrenia. Biol Psychiatry 23 : 210–2111, 1988
58) Waziri R : Correspondence; Glycine therapy of schizophrenia. Biol Psychiatry 40 : 685–686, 1996
59) 山本直樹，西川　徹：新たな抗精神病薬開発の未来．Schizophrenia Frontier 2 : 99–106, 2001

*　　*　　*

Available online at www.sciencedirect.com
ScienceDirect
ELSEVIER
Biochemical and Biophysical Research Communications 355 (2007) 385–391
BBRC
www.elsevier.com/locate/ybbrc

Structural basis of D-DOPA oxidation by D-amino acid oxidase: Alternative pathway for dopamine biosynthesis

Tomoya Kawazoe [a], Hideaki Tsuge [a,b], Takahito Imagawa [b], Kenji Aki [b], Seiki Kuramitsu [c,d], Kiyoshi Fukui [a,*]

[a] *The Institute for Enzyme Research, The University of Tokushima, 3-18-15 Kuramoto, Tokushima 770-8503, Japan*
[b] *Institute for Health Sciences, Tokushima Bunri University, 180 Nishihama, Yamashiro, Tokushima 770-8514, Japan*
[c] *RIKEN SPring-8 Center, Harima Institute, 1-1-1 Kohto, Sayo-cho, Hyogo 679-5148, Japan*
[d] *Department of Biology, Graduate School of Science, Osaka University, 1-1 Machikaneyama-cho, Toyonaka, Osaka 560-0043, Japan*

Received 23 January 2007
Available online 8 February 2007

Abstract

D-Amino acid oxidase (DAO) degrades the gliotransmitter D-serine, a potent endogenous ligand of *N*-methyl-D-aspartate type glutamate receptors. It also has been suggested that D-DOPA, the stereoisomer of L-DOPA, is oxidized by DAO and then converted to dopamine via an alternative biosynthetic pathway. Here, we provide direct crystallographic evidence that D-DOPA is readily fitted into the active site of human DAO, where it is oxidized by the enzyme. Moreover, our kinetic data show that the maximal velocity for oxidation of D-DOPA is much greater than for D-serine, which strongly supports the proposed alternative pathway for dopamine biosynthesis in the treatment of Parkinson's disease. In addition, determination of the structures of human DAO in various states revealed that the conformation of the hydrophobic VAAGL stretch (residues 47–51) to be uniquely stable in the human enzyme, which provides a structural basis for the unique kinetic features of human DAO.

Keywords: D-Amino acid oxidase; X-ray crystallography; D-DOPA; D-Serine; Dopamine; Parkinson's disease

D-Amino acid oxidase (DAO) (EC 1.4.3.3) was first identified by Hans Krebs in 1935 and was later recognized to be the first enzyme known to use FAD as a cofactor. DAO noncovalently binds FAD and catalyzes the oxidative deamination of D-amino acids to their corresponding imino acids with concomitant reduction of FAD. The reduced flavin is subsequently reoxidized by molecular oxygen generating H_2O_2, and the imino acid is released into the solvent, where it is nonenzymatically hydrolyzed, yielding the corresponding α-keto acid and ammonia. DAO exhibits its optimal activity toward neutral amino acids and marginal activity toward basic ones; acidic D-amino acids are oxidized by another flavoprotein, D-aspartate oxidase (for reviews, see [1–3]).

Discovered in 1993 [4], the DAO substrate D-serine is thought to be a gliotransmitter and an endogenous ligand for *N*-methyl-D-aspartate (NMDA) receptors in brain [5]. Moreover, evidence suggests that DAO, together with its activator, G72 protein, plays a key role in the pathophysiology of schizophrenia [6]. For instance, a major advance in the treatment of schizophrenia was achieved in the early 1950s with the introduction of chlorpromazine, a dopamine D2 receptor antagonist (for review, see [7]). But chlorpromazine also inhibits DAO by competing with FAD [8]. In that context, it is noteworthy that D-DOPA, the stereoisomer of L-DOPA, which is commonly used in the treatment of Parkinson's disease, is reportedly metabolized by DAO. In fact, when D-DOPA is administered, it is converted to dopamine via an alternative biosynthetic pathway

* Corresponding author. Fax: +81 88 633 7431.
E-mail address: kiyo@ier.tokushima-u.ac.jp (K. Fukui).

0006-291X/$ - see front matter © 2007 Elsevier Inc. All rights reserved.
doi:10.1016/j.bbrc.2007.01.181

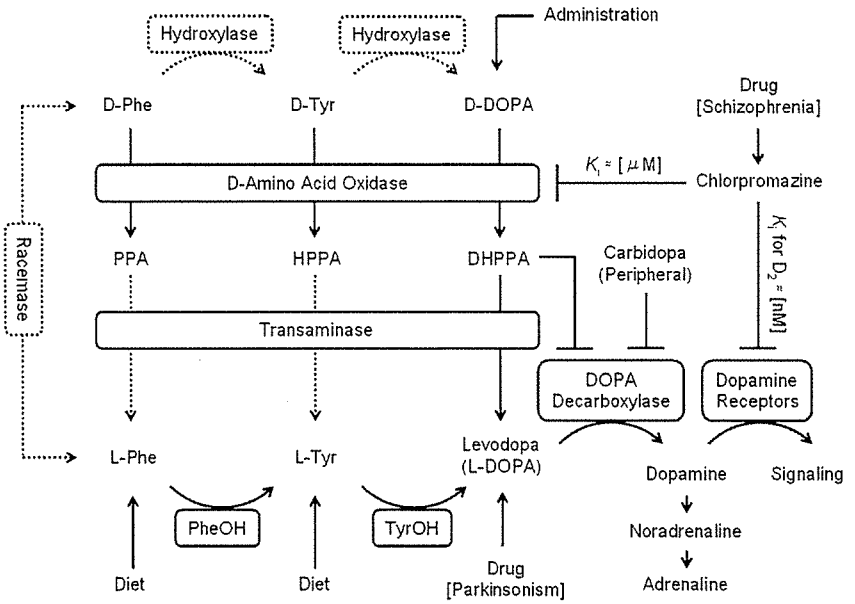

Scheme 1. General and alternative dopamine synthetic pathways. When administered, D-DOPA is converted to DHPPA by DAO, after which the α-keto acid is transaminated to L-DOPA [9,10]. Hypothetical reactions are shown as dashed lines. Phenylalanine racemase, which converts L-Phe to D-Phe, is known to exist in *Bacillus brevis* [30]. DHPPA, dihydroxyphenylpyruvic acid; PheOH, phenylalanine hydroxylase; TyrOH, tyrosine hydroxylase.

([9,10]; summarized in Scheme 1). Thus, the potential clinical importance of DAO in humans (hDAO) highlights the need for structural and functional analyses of this enzyme, as inhibitors acting selectively on hDAO are being intensively sought for clinical purposes [11].

We recently determined the crystal structure of hDAO in complex with benzoate [12]. Our findings showed that the hydrophobic VAAGL stretch (residues 47–51) located at the *si*-face of the flavin ring assumes a conformation different from that of porcine DAO (pDAO) ([13,14]). Upon reduction of the enzyme, the VAAGL stretch in pDAO changes its conformation, eliminating an H-bond between the flavin N5 atom and Ala49 [15]. However, because only a single structural form of hDAO is available, whether such a conformational shift also occurs in hDAO remained unknown. To address that question, we determined the crystal structures of the substrate-free form of hDAO, the reduced form in complex with imino-serine, and the oxidized form in complex with *o*-aminobenzoate. Moreover, because it is thought to be important for clinical applications, we assessed the capacity of hDAO to catalyze the oxidation of D-DOPA and analyzed the structure of hDAO in complex with imino-DOPA.

Materials and methods

Production and purification. Recombinant hDAO was produced and purified using essentially the same procedures described previously [12]. However, as described in Results and discussion section, changing the induction conditions from 0.1 mM IPTG ($OD_{600} = 0.6$) to 1 mM IPTG ($OD_{600} = 2.0$) significantly improved the hDAO production, enabling us to obtain about 97 mg of purified hDAO from a 4-L culture (Supplemental Table 1 and Supplemental Fig. 1a).

Kinetic analyses. Before the kinetic analyses, the purified holoenzyme in complex with benzoate was free from FAD and benzoate by dialysis against 50 mM Na phosphate (pH 6.8) containing 1 M KBr [16], and the concentration of the apoenzyme was determined using an extinction coefficient of 73 $mM^{-1}cm^{-1}$ at 280 nm [17]. The apoenzyme was then incubated with FAD for 1 h at 20 °C, after which the resultant substrate-free holoenzyme was used for the measurement. DAO activity was measured using an oxygraphic assay with a Clark oxygen electrode (Gilson, model 5/6 Oxygraph). The standard reaction mixture contained 50 μM FAD in a total volume of 1.8 ml. The reactions were initiated by addition of hDAO (5 μg) and carried out in 50 mM Na pyrophosphate buffer (pH 8.3) at 25 °C.

Crystallization and data collection. Crystals of hDAO were prepared using the hanging drop vapor diffusion method under previously reported conditions [12]. Yellow crystals of the substrate-free holoenzyme grew to an average size of 0.1 × 0.1 × 0.4 mm in 10 days at 20 °C (Supplemental Fig. 1b). Colorless crystals of the reduced enzyme in complex with imino-Ser were prepared by soaking the substrate-free crystals with 100 mM D-Ser (Supplemental Fig. 1c). After soaking for a few minutes to a few hours (depending upon the reservoir conditions and crystal sizes), the yellow crystals became colorless, indicating the conversion of D-Ser to imino-Ser. Colorless crystals of hDAO in complex with imino-DOPA were similarly prepared by soaking the substrate-free crystals with 75 mM D-DOPA. Crystals of the reduced enzyme (imino-Ser complex or imino-DOPA complex) remained colorless after the data collection. Crystals of oxidized hDAO in complex with *o*-aminobenzoate were prepared by cocrystallization. The apoenzyme was preincubated with a mixture of 2 mM FAD and 200 mM *o*-aminobenzoate for 1 h at 20 °C. Brownish-yellow crystals were obtained after 10 days at 20 °C. The data collection statistics are summarized in Table 1. Data were processed using the HKL2000 software package [18].

Structural determination and refinement. The refinement statistics are summarized in Table 2. Structural determination and refinement calculations were carried out using the CCP4 suite [19]. The structure was solved by molecular replacement using hDAO dimer as a search model. The dictionary files for small molecules (FAD, *o*-aminobenzoate, D-Ser, and D-Tyr) were obtained from HIC-UP, the Hetero-compound Information Centre—Uppsala (for review, see [20]). The library files for imino-Ser and imino-DOPA were generated with CCP4 Sketcher using D-Ser or D-Tyr as the model. The topology and parameter files for imino-Ser and imino-DOPA were generated using XPLO2D (for review, see [21]). FAD and ligand (imino-Ser, imino-DOPA or *o*-aminobenzoate) were built into the

Table 1
Data collection statistics

	PDB code (ligand)			
	2E48 (substrate-free)	2E49 (imino-Ser)	2E4A (*o*-AB)	2E82 (imino-DOPA)
Redox state of FAD	Oxidized	Reduced	Oxidized	Reduced
Wavelength (Å)	1.0			
Temperature (K)	100	100	297	100
Unit cell (Å)	$a = 149.652$	$a = 149.661$	$a = 151.392$	$a = 150.015$
	$b = 181.727$	$b = 181.745$	$b = 185.042$	$b = 181.886$
	$c = 50.815$	$c = 50.717$	$c = 51.577$	$c = 50.916$
Space group	$P2_12_12$			
Resolution (Å)	50.00–2.90 (3.00–2.90)	50.00–3.20 (3.31–3.20)	50.00–2.60 (2.69–2.60)	40.00–2.70 (2.80–2.70)
No. of reflections	31,102 (2,617)	23,223 (2,131)	45,267 (4,414)	38,354 (3,546)
Completeness (%)	97.3 (82.9)	97.5 (92.3)	98.8 (98.2)	97.5 (92.2)
Linear R_{fac}	0.102 (0.245)	0.133 (0.223)	0.085 (0.331)	0.068 (0.207)
I/sigma	5.9	7.2	9.0	14.6
Redundancy	3.8 (2.7)	3.7 (3.4)	3.1 (2.5)	6.0 (5.5)
Solvent content (%)	42.6	42.5	45.1	42.9
Matthews coeff. (Å^3/Da)	2.2	2.2	2.3	2.2
No. of subunits per asymm. unit	4			

Values in parentheses are for the highest resolution shell.
o-AB, *o*-aminobenzoate.

Table 2
Refinement statistics

	PDB code (ligand)			
	2E48 (substrate-free)	2E49 (imino-Ser)	2E4A (*o*-AB)	2E82 (imino-DOPA)
Resolution (Å)	50.00–2.90 (2.96–2.90)	50.00–3.20 (3.28–3.20)	50.00–2.60 (2.67–2.60)	40.00–2.70 (2.77–2.70)
No. of reflections	29,480	21,972	42,932	36,386
No. of reflections (R-free)	1,578	1,187	2,287	1,918
R-work (%)	21.0	22.1	21.0	21.0
R-free (%)	25.9	27.6	24.4	25.4
No. of non-H atoms				
Protein	10,932			
FAD	212			
Ligand	—	28	40	56
Water	134	112	106	126
Mean B value (Å^2)	33.7	40.8	39.9	37.1
RMS deviations				
Bond lengths (Å)	0.010	0.014	0.010	0.012
Bond angles (°)	1.347	1.506	1.400	1.479
Ramachandran plot (%)				
Most favored	85.8	80.3	89.4	85.1
Additionally allowed	13.4	18.9	10.2	14.5
Generously allowed	0.8	0.8	0.4	0.3
Disallowed	0.0	0.0	0.0	0.0

o-AB, *o*-aminobenzoate.

difference electron density map using strict noncrystallographic symmetry. Refinement was carried out using Refmac5 [22] and CNS [23]. The final model consisted of residues 1–340 for each of the four hDAO subunits in the asymmetric unit. After the final round of refinement, the stereochemistry of the structure was assessed using PROCHECK, taking particular care with the conformation of the VAAGL stretch (residues 47–51). The structures were confirmed with an omit map using a simulated annealing method after omitting the VAAGL stretch. To further confirm the structure, we collected four independent data sets for the substrate-free holoenzyme (2.9–3.3 Å), four data sets for the reduced form in complex with imino-Ser or imino-DOPA (2.7–3.2 Å) and three data sets for the oxidized form in complex with *o*-aminobenzoate (2.6–3.2 Å), and confirmed that the structures were essentially the same among the respective data sets (data not shown).

Results and discussion

Induction conditions are critical for effective production of recombinant hDAO

With an estimated expression level of only about 1 mg of enzyme per liter of culture, isolation of hDAO has been described as a very difficult task [17]. To prepare hDAO in amounts sufficient for crystallographic analysis, we investigated a wide range of production conditions. Of particular interest to us was the report from Pollegioni et al. indicating that expression of recombinant pDAO was

markedly enhanced when induction was carried out by adding 1 mM IPTG to relatively dense cell cultures ($OD_{600} = 2.8$) [24]. They suggested that these conditions were necessary because induction of DAO could be toxic to the *E. coli* cells, depending on the phase of their growth cycle. This report prompted us to apply similar conditions for the production of hDAO. We induced expression of the cloned gene using 1 mM IPTG in cultures with an OD_{600} of 2.0, which provided 46 g of wet cells from 4 liters of culture. Starting with this material, we were ultimately able to purify 97 mg of enzyme to 95% purity with an overall purification yield of 56% (Supplemental Table 1 and Supplemental Fig. 1a). This approach thus provided us with enough enzyme to crystallize hDAO in several states and enabled us to determine the structures of the substrate-free form, the reduced form in complex with imino-Ser or imino-DOPA, and the oxidized form in complex with *o*-aminobenzoate (Tables 1 and 2).

hDAO more actively oxidizes D-DOPA than previously identified substrates

Parkinson's disease is a chronic, progressive neurological disorder characterized by tremor, bradykinesia, rigidity, and postural instability. As summarized in Scheme 1, human cells synthesize dopamine from L-DOPA, which is derived from dietary tyrosine or phenylalanine (for review, see [25]). Because exogenous L-DOPA is converted to dopamine, its administration in combination with a peripheral DOPA decarboxylase inhibitor (carbidopa) remains the most effective symptomatic treatment for Parkinson's disease (for review, see [26]). When D-DOPA (Fig. 1A), the stereoisomer of L-DOPA, is administered, it is converted to dihydroxyphenylpyruvic acid (DHPPA) by DAO, which is followed by transamination from the α-keto acid to L-DOPA via what is known as the alternative pathway for dopamine biosynthesis ([9,10]; summarized in Scheme 1). Indeed, the slower utilization of D-DOPA, as well as the longer retention of its metabolites in brain [27], makes

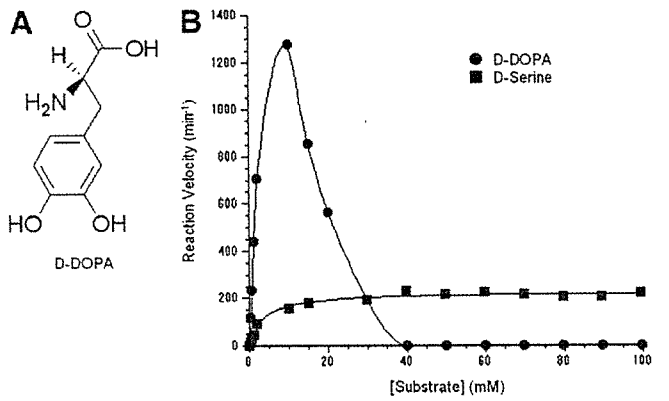

Fig. 1. D-DOPA is oxidized by purified hDAO in a manner different from D-Ser. (A) Chemical structure of D-DOPA. (B) Reaction velocity versus substrate concentration for the hDAO-catalyzed oxidation of D-DOPA or D-Ser.

the combination of the two isomers a more efficacious treatment for Parkinson's disease than L-DOPA alone [28].

To investigate the role of hDAO in the alternative pathway for dopamine biosynthesis, we first assessed the enzyme's ability to catalyze oxidation of D-DOPA. Unlike D-Ser, D-DOPA induced substrate inhibition at high concentrations (Fig. 1B). There appear to be three possible scenarios that could account for the observed substrate inhibition: (i) while substrate D-DOPA is bound to the active site, a second D-DOPA molecule binds to the active site in an orientation that makes progression of the reaction unlikely; (ii) a second D-DOPA binds to a location other than the active site, resulting in allosteric inhibition of the enzyme; and (iii) at high concentrations, D-DOPA forms homo-oligomers, thereby reducing its effective concentration in the solution. Of those three, the kinetics suggests the first is most likely. Moreover, the estimated inhibition constant (K_{is}) for the second D-DOPA had a value of 0.5 mM, as compared to a K_m value of 1.5 mM for the first substrate D-DOPA (Table 3). We therefore suggest that at high D-DOPA concentrations unproductive complexes are formed at the active site, but with a K_{is}/K_{ms} ratio of 0.3, this inhibition is physiologically irrelevant.

Importantly, at low concentrations, D-DOPA is oxidized by hDAO with a maximal velocity of 1300 min^{-1} (Table 3), which is significantly greater than the velocity seen with any previously identified hDAO substrate [29]. Indeed, D-DOPA showed a 14-fold higher k_{cat}/K_m value than D-Ser (Table 3), indicating D-DOPA to be the preferred substrate for hDAO. This finding is consistent with the proposal that when D-DOPA is administered, it is degraded by DAO, which ultimately leads to the production of dopamine via an alternative biosynthetic pathway [28]. We also examined the ability of hDAO to catalyze oxidation of D-Tyr and D-Phe, stereoisomers of two dopamine precursors (Scheme 1), and found that it oxidized both in a manner similar to D-DOPA (both showed substrate inhibition at high concentrations), though the turnover rates and k_{cat}/K_m values were lower (Table 3). Although phenylalanine racemase, which converts L-Phe to D-Phe, has been identified in *Bacillus brevis* [30], to our knowledge humans do not synthesize D-Phe. But when administered to humans, D-Phe potentiates analgesia (pain relief) and eases depression by inhibiting enkephalinase, which degrades enkephalin peptides, leading to the activation of the opioid delta receptors ([31,32], and for review, see [33]). These findings, together with our kinetic data, suggest that exogenously administered D-amino acids are able to act as effective

Table 3
Substrate preferences of hDAO: apparent kinetic values

	M_W (Da)	k_{cat} (min^{-1})	K_m (mM)	k_{cat}/K_m ($s^{-1}M^{-1}$)
D-Ser	105.09	240	3.9	1.0×10^3
D-Phe	165.19	930	1.2	1.3×10^4
D-Tyr	181.19	890	1.1	1.3×10^4
D-DOPA	197.19	1300	1.5	1.4×10^4

neuromodulators and highlight the importance of DAO for metabolism of many of these molecules.

Structure of the hDAO-imino-DOPA complex

In order to investigate the structural basis for the different activities of hDAO toward D-DOPA and D-Ser, we determined the structure of the enzyme in complex with imino-DOPA or imino-Ser. By soaking crystals of substrate-free (yellow) hDAO with excess amounts of D-Ser, we were able to obtain crystals of the reduced form (colorless) of the enzyme (Supplemental Fig. 1c), indicating that D-Ser is oxidized in crystal to produce the corresponding imino acid. The electron density map (Fig. 2A) shows that imino-Ser is bound within the active site of hDAO, further confirming that exogenously applied D-Ser is converted to imino-Ser by the enzyme in crystal. We next examined the mode by which imino-DOPA is bound within the active site of hDAO. From the data shown in Fig. 1B, oxidation of D-DOPA would not be expected to occur at concentrations higher than 40 mM. Nonetheless, by soaking crystals of the substrate-free enzyme in 75 mM D-DOPA, we were able to obtain colorless (reduced state) crystals, which is consistent with the earlier observation that the enzyme's reactivity in solution does not reflect its reactivity in crystal [15].

The electron density map clearly identified the imino-DOPA molecule within the active site of each of the four hDAO subunits in the asymmetric unit (Fig. 2B). The determined structure revealed that the bulky side chain of imino-DOPA forms H-bonds and makes hydrophobic contacts with the residues comprising the active site cavity. In Fig. 2C, the active sites of the imino-DOPA and imino-Ser complexes were superimposed, revealing that in contrast to imino-Ser, the aromatic ring of imino-DOPA forms H-bonds with Gln53 and His217 at distances of 3.2 and 3.4 Å, respectively. This suggests that these residues are involved in determining the substrate specificity and, presumably, are responsible for the different activities of hDAO toward D-DOPA and D-Ser.

A single conformation is unique to the VAAGL stretch in hDAO

We previously determined the structure of the oxidized form of hDAO in complex with benzoate and observed

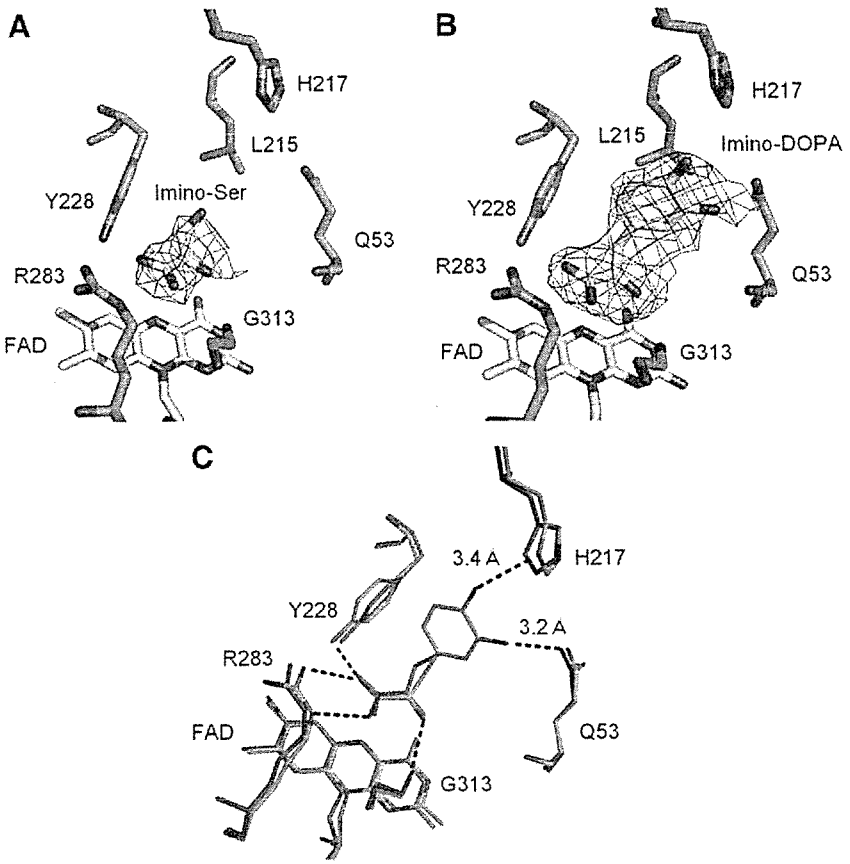

Fig. 2. Structural evidence of D-DOPA oxidation by hDAO and its ligand binding mode within the active site. (A) The active site of reduced hDAO in complex with imino-Ser (carbons in white). The electron density of imino-Ser (an $F_o - F_c$ map contoured at 1.0 sigma) is shown as blue mesh. The hDAO residues (carbons in green) and FAD (carbons in yellow) are shown in sticks in (A) and (B). For clarity, Tyr224 is not shown. (B) Imino-DOPA (carbons in white) was found to bind within the active site of hDAO. The electron density of imino-DOPA (an $F_o - F_c$ map contoured at 1.0 sigma) is shown in blue mesh. (C) The superimposition of the active sites of the imino-DOPA (carbons in green) and imino-Ser (carbons in magenta) complexes. The superimposition revealed that the bulky side chain of imino-DOPA forms additional H-bonds with Gln53 and His217. H-bonds are shown in dashed lines. In all of the figures, structural models were prepared using PyMOL (http://www.pymol.org).

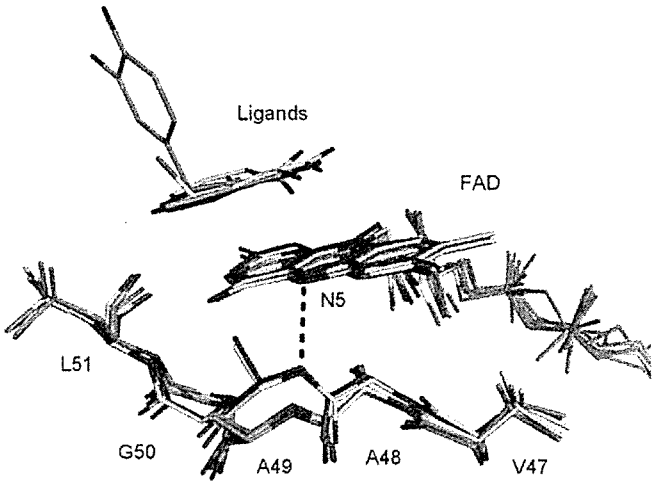

Fig. 3. The conformation of the VAAGL stretch (residues 47–51) is uniquely stable in hDAO. The VAAGL stretches of the substrate-free form (carbons in salmon), the reduced form in complex with imino-DOPA (carbons in green) or imino-Ser (carbons in white), and the oxidized form in complex with *o*-aminobenzoate (carbons in cyan) were superimposed. VAAGL stretches from oxidized pDAO ([13]: PDB code 1KIF in magenta; [14]: PDB code 1VE9 in yellow) are also superimposed, highlighting the difference of their conformation from that of hDAO.

that the conformation of the VAAGL stretch (residues 47–51), which is located at the *si*-face of the flavin ring, differs from that in pDAO [12]. Furthermore, the conformation of the VAAGL stretch in the reduced form of hDAO remained unknown. In fact, a conformational change occurs upon transition from the oxidized to the reduced form of pDAO, resulting in the loss of a H-bond between the flavin N5 atom and the backbone N atom of Ala49 [15].

Fig. 3 shows a superimposition of the VAAGL stretches from the substrate-free and reduced forms of hDAO. In addition, to reproduce the stretch conformation in the oxidized form, we determined the structure of hDAO in complex with *o*-aminobenzoate, which is also shown superimposed in Fig. 3. In contrast to pDAO, VAAGL stretches in hDAO assumed a single conformation in all three forms examined. The context-dependent conformational variability of a structurally ambivalent peptide (SAP; in this case VAAGL) is thought to reflect the local and/or global context of the protein [34]. Given that the 13 local residues, including the SAP region (TTTD-VAAGL-WQPY; residues 43–55), are completely conserved between the human and porcine enzymes, we suggest the global context of hDAO restricts the VAAGL stretch to a single conformation, which provides a molecular basis for the enzyme's weaker FAD binding and slower rate of flavin reduction, as compared to pDAO [29].

Protein Data Bank accession codes

The atomic coordinates and structural factors for the substrate-free holoenzyme (code 2E48), imino-Ser complex (code 2E49), *o*-aminobenzoate complex (code 2E4A), and imino-DOPA complex (code 2E82) have been deposited in the Protein Data Bank, Research Collaboratory for Structural Bioinformatics, Rutgers University, New Brunswick, NJ (http://www.rcsb.org/).

Acknowledgments

We thank Nobuhiko Katunuma and Kayoko Komori for discussions. We also thank Akio Ebihara, Mayumi Kanagawa, and Yoshiaki Kitamura for their help in data collection at SPring-8 beamline BL26B1 and BL26B2. D-Cha, the database for crystallography with home-lab arrangement, was used for checking/collecting CCD images from the remote site. This work was supported in part by a Grant-in-Aid for Scientific Research and a Grant for the 21st Century COE Program from the Ministry of Education, Science, Sports and Culture of Japan, a Grant for Scientific Research from the Japan Society for the Promotion of Science, and a Research Grant from the Ministry of Health, Labor and Welfare of Japan. This work was also supported in part by the National Project on Protein Structural and Functional Analyses from the MEXT of Japan.

Appendix A. Supplementary data

Supplementary data associated with this article can be found, in the online version, at doi:10.1016/j.bbrc.2007.01.181.

References

[1] B. Curti, S. Ronchi, S.M. Pilone, D- and L-amino acid oxidases, in: F. Muller (Ed.), Chemistry and Biochemistry of Flavoenzymes, vol. III, CRC Press, Boca Raton, 1992, pp. 69–94, chapter 3.
[2] M.S. Pilone, D-Amino acid oxidase: new findings, Cell Mol. Life Sci. 57 (2000) 1732–1747.
[3] S. Ghisla, L. Pollegioni, D-amino acid oxidase: still new lessons from a seventy year old flavoprotein, in: T. Nishino et al. (Eds.), Flavins and Flavoproteins 2005, ARchiTect Inc., Japan, 2005, pp. 17–32.
[4] A. Hashimoto, T. Nishikawa, T. Oka, K. Takahashi, Endogenous D-serine in rat brain: *N*-methyl-D-aspartate receptor-related distribution and aging, J. Neurochem. 60 (1993) 783–786.
[5] J.P. Mothet, A.T. Parent, H. Wolosker, R.O. Brady Jr., D.J. Linden, C.D. Ferris, M.A. Rogawski, S.H. Snyder, D-serine is an endogenous ligand for the glycine site of the *N*-methyl-D-aspartate receptor, Proc. Natl. Acad. Sci. USA 97 (2000) 4926–4931.
[6] I. Chumakov, M. Blumenfeld, O. Guerassimenko, L. Cavarec, M. Palicio, H. Abderrahim, L. Bougueleret, C. Barry, H. Tanaka, P. La Rosa, et al., Genetic and physiological data implicating the new human gene G72 and the gene for D-amino acid oxidase in schizophrenia, Proc. Natl. Acad. Sci. USA 99 (2002) 13675–13680.
[7] A. Sawa, S.H. Snyder, Schizophrenia: diverse approaches to a complex disease, Science 296 (2002) 692–695.
[8] K. Yagi, T. Nagatsu, T. Ozawa, Inhibitory action of chlorpromazine on the oxidation of D-amino-acid in the diencephalon part of the brain, Nature 177 (1956) 891–892.
[9] H. Shindo, T. Maeda, Studies on the metabolism of D- and L-isomers of 3,4-dihydroxyphenylalanine (DOPA). VI. Metabolism of D-DOPA in rat kidney, Chem. Pharm. Bull. (Tokyo) 22 (1974) 1721–1731.
[10] F. Karoum, W.J. Freed, L.W. Chuang, E. Cannon-Spoor, R.J. Wyatt, E. Costa, D-dopa and L-dopa similarly elevate brain dopamine and produce turning behavior in rats, Brain Res. 440 (1988) 190–194.
[11] P.E. Brandish, C.S. Chiu, J. Schneeweis, N.J. Brandon, C.L. Leech, O. Kornienko, E.M. Scolnick, B. Strulovici, W. Zheng, A cell-based

ultra-high-throughput screening assay for identifying inhibitors of D-amino acid oxidase, J. Biomol. Screen. 11 (2006) 481–487.
[12] T. Kawazoe, H. Tsuge, M.S. Pilone, K. Fukui, Crystal structure of human D-amino acid oxidase: context-dependent variability of the backbone conformation of the VAAGL hydrophobic stretch located at the si-face of the flavin ring, Protein Sci. 15 (2006) 2708–2717.
[13] A. Mattevi, M.A. Vanoni, F. Todone, M. Rizzi, A. Teplyakov, A. Coda, M. Bolognesi, B. Curti, Crystal structure of D-amino acid oxidase: a case of active site mirror-image convergent evolution with flavocytochrome b2, Proc. Natl. Acad. Sci. USA 93 (1996) 7496–7501.
[14] H. Mizutani, I. Miyahara, K. Hirotsu, Y. Nishina, K. Shiga, C. Setoyama, R. Miura, Three-dimensional structure of pig kidney D-amino acid oxidase at 3.0 Å resolution, J. Biochem. (Tokyo) 120 (1996) 14–17.
[15] F. Todone, M.A. Vanoni, A. Mozzarelli, M. Bolognesi, A. Coda, B. Curti, A. Mattevi, Active site plasticity in D-amino acid oxidase: a crystallographic analysis, Biochemistry 36 (1997) 5853–5860.
[16] V. Massey, B. Curti, A new method of preparation of D-amino acid oxidase apoprotein and a conformational change after its combination with flavin adenine dinucleotide, J. Biol. Chem. 241 (1966) 3417–3423.
[17] A.A. Raibekas, K. Fukui, V. Massey, Design and properties of human D-amino acid oxidase with covalently attached flavin, Proc. Natl. Acad. Sci. USA 97 (2000) 3089–3093.
[18] Z. Otwinowski, W. Minor, Processing of X-ray diffraction data collected in oscillation mode, in: C.W. CarterJr., R.M. Sweet (Eds.), Methods in Enzymology, Macromolecular Crystallography, part A, vol. 276, Academic Press, New York, 1997, pp. 307–326.
[19] Collaborative Computational Project, Number 4, The CCP4 suite: programs for protein crystallography, Acta Crystallogr. D: Biol. Crystallogr. 50 (1994) 760–763.
[20] G.J. Kleywegt, T.A. Jones, Databases in protein crystallography, Acta Crystallogr. D: Biol. Crystallogr. 54 (Pt 6 Pt 1) (1998) 1119–1131.
[21] G.J. Kleywegt, K. Henrick, E.J. Dodson, D.M. van Aalten, Pound-wise but penny-foolish: how well do micromolecules fare in macromolecular refinement? Structure 11 (2003) 1051–1059.
[22] G.N. Murshudov, A.A. Vagin, E.J. Dodson, Refinement of macromolecular structures by the maximum-likelihood method, Acta Crystallogr. D: Biol. Crystallogr. 53 (1997) 240–255.
[23] A.T. Brunger, P.D. Adams, G.M. Clore, W.L. DeLano, P. Gros, R.W. Grosse-Kunstleve, J.S. Jiang, J. Kuszewski, M. Nilges, N.S. Pannu, R.J. Read, L.M. Rice, T. Simonson, G.L. Warren, Crystallography and NMR system: a new software suite for macromolecular structure determination, Acta Crystallogr. D: Biol. Crystallogr. 54 (1998) 905–921.
[24] L. Pollegioni, K. Fukui, V. Massey, Studies on the kinetic mechanism of pig kidney D-amino acid oxidase by site-directed mutagenesis of tyrosine 224 and tyrosine 228, J. Biol. Chem. 269 (1994) 31666–31673.
[25] M.J. Aminoff, Treatment of Parkinson's disease, West J. Med. 161 (1994) 303–308.
[26] Y. Agid, Levodopa: is toxicity a myth? Neurology 50 (1998) 858–863.
[27] H. Shindo, E. Nakajima, K. Kawai, N. Miyakoshi, K. Tanaka, Studies on the metabolism of D- and L-isomers of 3,4-dihydroxyphenylalanine (DOPA). 3. Absorption, distribution and excretion of D- and L-DOPA-14C in rats following intravenous and oral administration, Chem. Pharm. Bull. (Tokyo) 21 (1973) 817–825.
[28] J. Moses, A. Siddiqui, P.B. Silverman, Sodium benzoate differentially blocks circling induced by D-and L-dopa in the hemi-parkinsonian rat, Neurosci. Lett. 218 (1996) 145–148.
[29] G. Molla, S. Sacchi, M. Bernasconi, M.S. Pilone, K. Fukui, L. Pollegioni, Characterization of human D-amino acid oxidase, FEBS Lett. 580 (2006) 2358–2364.
[30] M. Yamada, K. Kurahashi, Adenosine triphosphate and pyrophosphate dependent phenylalanine racemase of Bacillus brevis Nagano, J. Biochem. (Tokyo) 63 (1968) 59–69.
[31] S. Ehrenpreis, D-Phenylalanine and other enkephalinase inhibitors as pharmacological agents: implications for some important therapeutic application, Acupunct. Electrother. Res. 7 (1982) 157–172.
[32] L.M. Halpern, W.K. Dong, D-phenylalanine: a putative enkephalinase inhibitor studied in a primate acute pain model, Pain 24 (1986) 223–237.
[33] A.L. Russell, M.F. McCarty, DL-phenylalanine markedly potentiates opiate analgesia - an example of nutrient/pharmaceutical up-regulation of the endogenous analgesia system, Med. Hypotheses 55 (2000) 283–288.
[34] I.B. Kuznetsov, S. Rackovsky, On the properties and sequence context of structurally ambivalent fragments in proteins, Protein Sci. 12 (2003) 2420–2433.

Crystal structure of human D-amino acid oxidase: Context-dependent variability of the backbone conformation of the VAAGL hydrophobic stretch located at the *si*-face of the flavin ring

TOMOYA KAWAZOE,[1] HIDEAKI TSUGE,[1,2] MIRELLA S. PILONE,[3] AND KIYOSHI FUKUI[1]

[1]The Institute for Enzyme Research, The University of Tokushima, 3-18-15 Kuramoto, Tokushima 770-8503, Japan
[2]Institute for Health Sciences, Tokushima Bunri University, 180 Nishihama, Yamashiro, Tokushima 770-8514, Japan
[3]Department of Biotechnology and Molecular Sciences, University of Insubria, 21100 Varese, Italy

(RECEIVED July 21, 2006; FINAL REVISION September 6, 2006; ACCEPTED September 6, 2006)

Abstract

In the brain, the extensively studied FAD-dependent enzyme D-amino acid oxidase (DAO) degrades the gliotransmitter D-serine, a potent activator of *N*-methyl-D-aspartate type glutamate receptors, and evidence suggests that DAO, together with its activator G72 protein, may play a key role in the pathophysiology of schizophrenia. Indeed, its potential clinical importance highlights the need for structural and functional analyses of human DAO. We recently succeeded in purifying human DAO, and found that it weakly binds FAD and shows a significant slower rate of flavin reduction compared with porcine DAO. However, the molecular basis for the different kinetic features remains unclear because the active site of human DAO was considered to be virtually identical to that of porcine DAO, as would be expected from the 85% sequence identity. To address this issue, we determined the crystal structure of human DAO in complex with a competitive inhibitor benzoate, at a resolution of 2.5 Å. The overall dimeric structure of human DAO is similar to porcine DAO, and the catalytic residues are fully conserved at the *re*-face of the flavin ring. However, at the *si*-face of the flavin ring, despite the strict sequence identity, a hydrophobic stretch (residues 47–51, VAAGL) exists in a significantly different conformation compared with both of the independently determined porcine DAO–benzoate structures. This suggests that a context-dependent conformational variability of the hydrophobic stretch accounts for the low affinity for FAD as well as the slower rate of flavin reduction, thus highlighting the unique features of the human enzyme.

Keywords: D-amino acid oxidase; *Homo sapiens*; X-ray crystallography; structurally ambivalent peptides; conformational variability

D-amino acid oxidase (DAO) (EC 1.4.3.3) was first identified by Hans Krebs in 1935 and was later recognized to be the first enzyme known to use FAD as a cofactor (Krebs 1935). DAO noncovalently binds FAD as a prosthetic group and catalyzes the oxidative deamination of D-amino acids to their corresponding imino acids with concomitant reduction of FAD. The reduced flavin is subsequently reoxidized by molecular oxygen generating H_2O_2, and the imino acid is released into the solvent where it nonenzymatically hydrolyzes, yielding the corresponding α-keto acid and ammonia. DAO exhibits its optimal activity toward neutral amino acids and marginal activity toward basic ones; acidic D-amino acids are oxidized by another flavoprotein, D-aspartate oxidase.

Reprint requests to: Kiyoshi Fukui, The Institute for Enzyme Research, The University of Tokushima, 3-18-15 Kuramoto, Tokushima 770-8503, Japan; e-mail: kiyo@ier.tokushima-u.ac.jp; fax: 81-88-633-7431.

Article published online ahead of print. Article and publication date are at http://www.proteinscience.org/cgi/doi/10.1110/ps.062421606.

DAO has been the subject of numerous studies over the past 70 yr, becoming a model for the class of flavin-dependent oxidases (for review, see Pilone 2000).

We previously determined the primary structures of DAO mRNAs isolated from pig kidney (Fukui et al. 1987) and human kidney (Momoi et al. 1988) and also detected a single mRNA species in the brain (Fukui et al. 1988). In addition, we isolated genomic clones of the entire gene from human placental genomic libraries and localized the human gene to chromosome 12 (Fukui and Miyake 1992). Two groups have independently reported the same crystal structure for pig kidney DAO in complex with a competitive inhibitor benzoate at resolutions of 2.6 Å (PDB code 1KIF; Mattevi et al. 1996) and 2.5 Å (PDB code 1VE9; Mizutani et al. 1996). The crystal structure of yeast DAO from *Rhodotorula gracilis* was determined at a higher resolution of 1.2 Å (Umhau et al. 2000), followed by the structure in complex with *o*-aminobenzoate (Pollegioni et al. 2002). These three-dimensional structures reported between 1996 and 2002 (six from porcine DAO, four from yeast DAO) have provided us with the molecular basis for our understanding of the mechanism via which this FAD-dependent enzyme acts (Mattevi et al. 1996; Mizutani et al. 1996, 2000; Miura et al. 1997; Todone et al. 1997; Pollegioni et al. 2002; for review, see Pilone 2000). Biochemical characterization of human DAO was not achieved until recently, mainly because of the difficulty of expressing it in a heterologous system such as *Escherichia coli* (Raibekas et al. 2000). However, we recently succeeded in purifying human DAO and investigating its main functional properties. We found that, in contrast to other known DAO enzymes, human DAO binds FAD only weakly and exists as a stable homodimer, even in the apoprotein form (Molla et al. 2006). The molecular basis for the difference between human DAO and other forms remains unclear because the three-dimensional structure of human DAO was considered to be virtually identical to that of the porcine enzyme, as would be expected from their 85% sequence identity.

From a clinical point of view, new data on the three-dimensional structure of human DAO are highly important because activation of human DAO by G72, which leads to enhanced degradation of the gliotransmitter D-serine, a potent activator of *N*-methyl-D-aspartate (NMDA)-type glutamate receptors, has been implicated in the pathophysiology of schizophrenia (Chumakov et al. 2002). Indeed, inhibitors acting selectively on human DAO are being intensively sought for clinical purposes (Brandish et al. 2006). Historically, a major advance in the treatment of schizophrenia was achieved in the early 1950s with the introduction of chlorpromazine, a dopamine D2 receptor antagonist (for review, see Sawa and Snyder 2002). It is noteworthy, however, that chlorpromazine also inhibits DAO activity by competing with FAD (Yagi et al. 1956). Because gene variants that result in expression of mutant DAO or G72 proteins have not been identified, it is conceivable that pathogenic mutations at the susceptibility loci or in regulatory regions (e.g., modified expression of DAO or G72) affect degradation of D-serine by DAO, leading to NMDA dysfunction. Our approach to modifying NMDA neurotransmission is to alter the availability of synaptic D-serine by modulating intracellular DAO activity. We previously confirmed that extracellular D-serine is metabolized by DAO expressed in astrocytes and that such activity can be inhibited by application of chlorpromazine (Park et al. 2006). In the present study, we determined the crystal structure of recombinant human DAO in complex with benzoate at a resolution of 2.5 Å. Comparison with the known structure of porcine DAO revealed a remarkable difference in the conformation of the VAAGL hydrophobic stretch, which is located at the *si*-face of the flavin ring.

Results and Discussion

Purification and crystallization of recombinant human DAO

With an estimated yield of as little as 1 mg of enzyme per liter of culture, human DAO has proven to be a difficult protein to express in recombinant form, making isolation of the pure enzyme a very difficult task (Raibekas et al. 2000). In contrast, 16 mg of recombinant porcine DAO can be obtained per liter of IPTG-induced culture (Setoyama et al. 1996). Nevertheless, we recently succeeded in purifying recombinant human DAO to 85% purity (estimated by SDS-PAGE) in amounts of ~4.2 mg of enzyme per liter of culture, with an overall purification yield of 60% (Molla et al. 2006). Although this work enabled us to functionally characterize the human enzyme, we were unable to produce crystals of human DAO (T. Kawazoe, H. Tsuge, and K. Fukui, unpubl.). In order to prepare enough enzyme for crystallization, we further explored a wide range of conditions including the IPTG concentration (Fig. 1A) and the purification steps (data not shown). As a result of this effort, we were ultimately able to purify 5.0 mg of enzyme per liter of culture to 95% purity (estimated by SDS-PAGE; Fig. 1B) with an overall purification yield of 55% (Table 1A).

To assess the functional characteristics of the purified enzyme, we used an oxygen electrode to detect the consumption of oxygen during catalysis (Table 1B). The gliotransmitter D-Ser, a potent physiological substrate of human DAO, was oxidized by the purified enzyme with an apparent affinity (K_m) of 3.6 mM, a value comparable to that of recombinant porcine DAO (Setoyama et al. 2002). Addition of excess benzoate completely inhibited the enzyme activity with an apparent K_i of 7 μM. Based

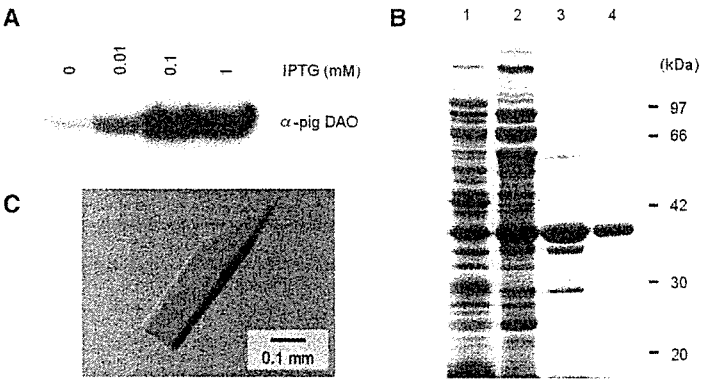

Figure 1. Purification and crystallization of recombinant human DAO. *(A)* Western blot of recombinant human DAO produced in *E. coli*. *(B)* SDS-PAGE of purified DAO isolated from *E. coli*. The gel (10%) was stained with Coomassie blue. (Lane *1*) Whole cell (containing 20 μg of protein), (lane 2) after heat treatment (59°C, 3 min) and 70% ammonium sulfate fractionation (20 μg of protein), (lane *3*) DEAE Sepharose CL-6B column eluate (5 μg of protein), (lane *4*) hydroxylapatite column eluate (2 μg of protein). Values indicate the molecular weight of the marker proteins: phosphorylase b (97 kDa), BSA (66 kDa), aldolase (42 kDa), carbonic anhydrase (30 kDa), and soybean trypsin inhibitor (20 kDa). *(C)* Crystal of human DAO.

on these results, we prepared and crystallized a ternary complex comprised of the purified enzyme bound with FAD and benzoate (Fig. 1C).

Overall structure of the human DAO holoenzyme in complex with benzoate

The crystal structure of human DAO was determined by molecular replacement of the porcine enzyme (PDB code 1AN9; 2.5 Å; Miura et al. 1997). The asymmetric unit contained four molecules of human DAO in the form of two homodimers. Basically, each of the four molecules showed the same conformation, and the overall dimeric structure of human DAO (Fig. 2A) was identical to the "head-to-head" structure of porcine DAO (Mattevi et al. 1996; Mizutani et al. 1996), but different from the "head-to-tail" structure of the yeast enzyme (Pollegioni et al. 2002). The C terminus of the human DAO subunit (residues 341–347) was not clear in the electron density map, which is indicative of the flexibility of this region. The human DAO subunit (residues 1–347; 39 kDa) contained one molecule of noncovalently bound FAD as a cofactor and one molecule of benzoate as an inhibitory substrate analog (Fig. 2B). The Dali score (Holm and Sander 1993) between the human and porcine DAO subunits was 54.2 (RMSD of 0.6 Å for 340 Cα pairs; 85% sequence identity), while that between the human and yeast DAO subunits was 39.1 (RMSD of 1.9 Å for 319 Cα pairs; 28% sequence identity). As shown in Figure 2C, the human DAO subunit contains 11 α-helices and 14 β-strands, which fold into two domains, the FAD-binding domain and the interface domain.

Among the 30 residues located at the dimer interface of human DAO, 10 (33%) differ from the corresponding residue in porcine DAO, while 20 (67%) are conserved (Fig. 3). Thus, the frequency of substitution at the dimer interface is higher than the overall substitution frequency (53 residues; 15%). As a consequence, the electrostatic

Table 1. *Purification and apparent kinetic parameters*

A. Purification of recombinant human DAO[a]

	Total activity (U)[c]	Total protein (mg)	Specific activity (U/mg)	Yield (%)	Purification (-fold)
Whole cell[b]	650	1700	0.4	100	1
Heat and $(NH_4)_2SO_4$	580	290	2.0	89	5
DEAE Sepharose	400	27	14.8	62	37
Hydroxylapatite	360	20	18.0	55	45

[a] Data represent a typical purification, which was repeated more than three times with similar results.
[b] Based on 30 g of *E. coli* cells from 4 L of culture.
[c] The amount of enzyme that consumes 1 μmol of O_2 per min at 25°C.

B. Apparent kinetic parameters

	k_{cat} (min^{-1})		K_m (mM)	
	Human	Pig[a]	Human	Pig[a]
D-Pro	900	1260	1.7	1.1
D-Ala	330	510	0.9	1.1
D-Ser	170	162	3.6	4.8
Gly	36	—	140	—
	Human		Pig[b]	
K_i for benzoate (μM)	7		9	

[a] Setoyama et al. 2002.
[b] Miyano et al. 1991.

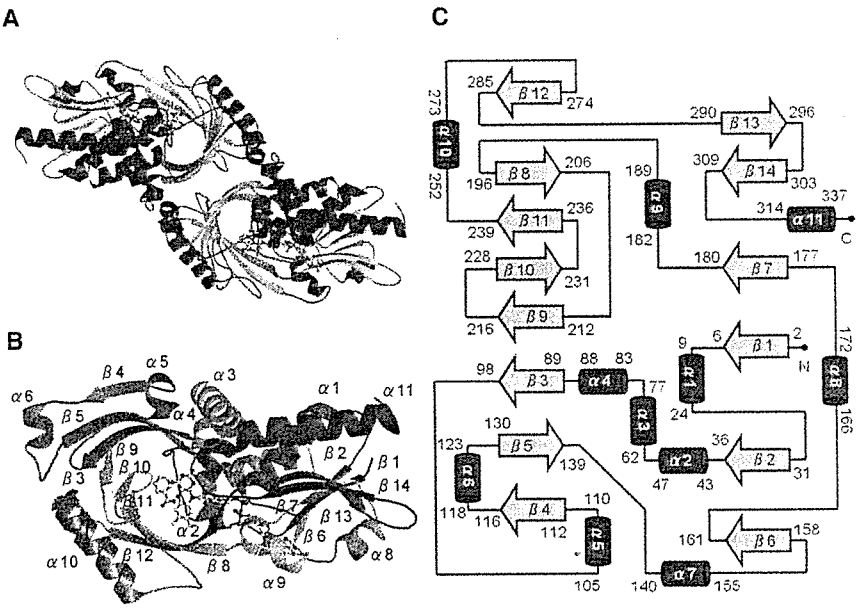

Figure 2. Overall structure of the human DAO holoenzyme in complex with benzoate. Structural models were prepared with PyMOL (http://www.pymol.org). FAD and benzoate are shown as ball-and-stick representations in *A* and *B*. *(A)* The DAO homodimer colored by secondary structure (helix in red, sheet in yellow, loop in green). *(B)* The DAO subunit colored spectrum in rainbow from the N terminus (blue) to the C terminus (red). Secondary structure elements are labeled. *(C)* Topology of the DAO subunit (helix in red, sheet in yellow). The cartoon was manually drawn based on the results of the TOPS algorithm (Michalopoulos et al. 2004). The DAO subunit consists of an FAD-binding domain (residues 1–88, 140–195, 286–340) and an interface domain (residues 89–139, 196–285). The first and the last residues are numbered for each secondary structure element.

surface potential at the dimer interface of human DAO differs from that of porcine DAO (Fig. 4): The dimer interface of the human enzyme is negatively charged, while that of porcine enzyme is positively charged. We previously reported that the oligomerization state of human DAO significantly differs from that of porcine DAO (Molla et al. 2006). In solution, within a concentration range of 1–24 mg/mL, the human enzyme is always found as a dimeric holoenzyme. In contrast, the porcine enzyme exhibits an oligomerization state that is dependent on the protein concentration. Moreover, in contrast to other known DAO enzymes, the human DAO homodimer is stable even in the apoprotein form, presumably reflecting the different surface properties at the dimer interface.

Context-dependent conformational variability of the VAAGL hydrophobic stretch

As expected from the 85% sequence identity, the active sites were conserved between the human and porcine enzymes at the *re*-face of the flavin ring (Fig. 5A). At the *si*-face of the flavin ring, however, we observed an important difference that was not expected, given the strict sequence identity at this region. In both enzymes, the *si*-face of the flavin ring is covered by a hydrophobic stretch (residues 47–51; VAAGL) (Mizutani et al. 1996), the conformation of which in human DAO differs significantly from both of the independently determined porcine DAO–benzoate complexes (Fig. 5B). The hydrophobic stretch is located inside the molecule, thus its conformation is considered to be rigid, as expected from the low average B-value of 44.6 $Å^2$ for the 29 stretch atoms (the average B-value for the overall protein atoms is 52.2 $Å^2$ as shown in Table 3, below). The human stretches were found to be in an identical conformation in all four molecules within the asymmetric unit (RMS of 0.23 ± 0.04 Å, among 29 atoms), which confirms the stability of the conformation, though a different conformation is favorable to the porcine DAO–benzoate structures. When compared with the overall structural similarity between the human and porcine enzymes (RMS of 0.40 Å for 215 Cα pairs comprising the all α-helices and β-sheets), the deviation of the hydrophobic stretch was evident from the RMS of 0.89 Å (Fig. 5C). This is surprising because the sequence of the hydrophobic stretch (VAAGL) is strictly conserved between the human and porcine enzymes. The stretch conformation in human DAO was confirmed by inspection of omit maps as described in the Materials and Methods section (Fig. 5D).

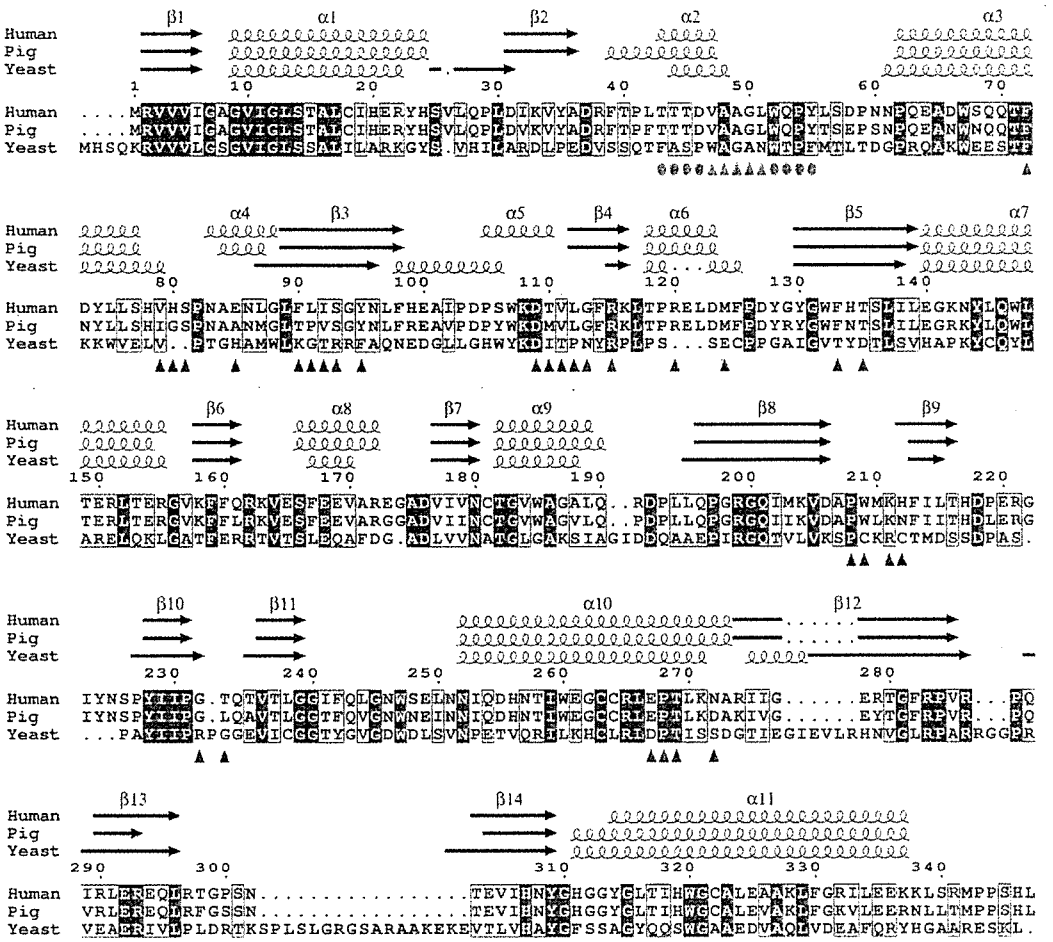

Figure 3. Structure-based sequence alignment of DAO. DAO sequences from human (Swiss-Prot no. P14920), pig (Swiss-Prot no. P00371), and yeast (Swiss-Prot no. P80324) were aligned using ClustalW 1.82 (Thompson et al. 1994) and colored using ESPript 2.2 (Gouet et al. 2003). White in a red box shows strict identity; red in a white box shows similarity within a group; and blue in a white box shows similarity across groups. The hydrophobic stretch is indicated (green triangles) with the residues locally conserved between the human and porcine enzymes (green circles). At the dimer interface of human DAO, 10 residues (red triangles) differ from the porcine enzyme, while 20 residues (blue triangles) are conserved.

Because it lacks a side chain, glycine is a conformationally flexible residue. This means that the hydrophobic stretch, which includes a glycine at position 50 (Fig. 3), is capable of adopting a variety of conformations depending upon the environment in which it is located. When the backbone conformations were evaluated in φ/ψ plots of the stretch residues in the human and porcine enzymes (Fig. 6), it was found that despite the strict sequence identity, the φ/ψ combinations of Ala48, Ala49, and Gly50 are diversified among the three DAO–benzoate structures, while those of Val47 and Leu51 are conserved. This means that the VAAGL hydrophobic stretch can be considered a structurally ambivalent peptide (SAP) comprised of five residues (Kuznetsov and Rackovsky 2003). It has been shown that a significant difference between two distinct conformations of the same SAP can be the result of both the overall sequence and the structural properties of the protein harboring the SAP (global context) or the sequence and structural properties of the SAP's flanking regions (local context). In the case of DAO, the conformational variability of the hydrophobic stretch appears to reflect the global context, as the 13 local residues, i.e., the hydrophobic stretch and its flanking regions (residues 43–55; TTTD-VAAGL-WQPY in Fig. 3) are conserved between the two enzymes.

Structural implication of the weak FAD binding in human DAO

We previously reported that the K_d of the FAD-apoenzyme complex is 40-fold higher for human DAO (8 ± 2 μM) than

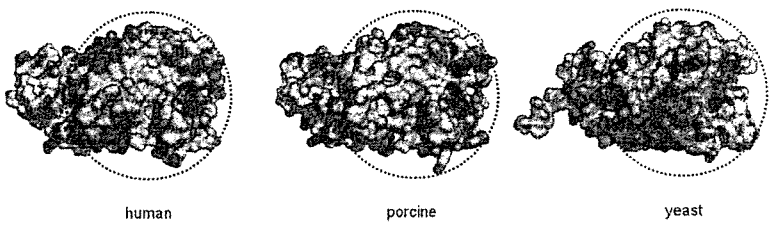

Figure 4. Electrostatic surface potential at the dimer interface. The dimer interface (shown within a dashed circle) of human DAO is negatively charged, while that of porcine DAO is positively charged. The corresponding surface area of the yeast DAO subunit is also shown in a dashed circle. The surface is colored from blue (positive) to red (negative). Only protein atoms were considered for surface calculation by GRASP (Nicholls et al. 1991). The electrostatic surface potential was scaled to a range between −10 kT and 10 kT e^{-1} (1 V = 38.94 kT e^{-1} at room temperature).

porcine DAO (0.2 μM) (Molla et al. 2006), and that the affinity for FAD is even stronger in yeast DAO (K_d = 0.02 μM) (summarized in Molla et al. 2006). The different affinities of the porcine and yeast enzymes for FAD have been attributed to the environment at the flavin O2 position (Pollegioni et al. 2002). In porcine DAO, the partial positive charge of a dipole induced by helix α11 (residues 311–337 in Fig. 3) is presumed to contribute to the stabilization of the negative charge of the reduced flavin (Mattevi et al. 1996), a feature that is absent in yeast DAO (Pollegioni et al. 2002). The flavin O2 atom is H-bonded to Thr317 in both the human and porcine enzymes (Fig. 5A), whereas in yeast DAO, the atom is tightly H-bonded to Tyr338 and Gln339 (Pollegioni et al. 2002). To confirm the effect of Thr317 on FAD binding, Setoyama et al. (2002) designed and expressed a porcine DAO T317A substitution mutant and noted that the mutant enzyme had a lower affinity for FAD. On the other hand, the different affinities for FAD of the porcine and human enzymes cannot be explained by the Thr317 position, given the overall structural conservation at the *re*-face of the flavin ring (Fig. 5A).

In order to provide a structural basis for the observed kinetic difference between human and porcine DAO, we compared the FAD-binding patterns of the two enzymes. Aside from the conformation of the hydrophobic stretch, no remarkable differences were observed, at least within 6 Å of FAD, which indicates that the hydrophobic stretch plays an important role in determining the affinity for FAD. As compared with porcine DAO, the hydrophobic stretch in the human enzyme is shifted away from the FAD, resulting in the loss of the H-bond between the flavin N5 atom and the backbone N atom of Ala49 with the distance of 3.9 Å (Fig. 5B).

A noticeable shift in the hydrophobic stretch also occurs in the reduced state of porcine DAO when the enzyme is complexed with the reaction product imino tryptophan (PDB code 1DDO; 3.1 Å; Todone et al. 1997) and in the structure of the purple intermediate (a complex between the dehydrogenated product and the reduced form of DAO) (PDB code 1EVI; 2.5 Å; Mizutani et al. 2000) (Fig. 5B). In the porcine enzyme, the length of the H-bond between the flavin N5 atom and the Ala49 backbone N atom is 3.0 Å in the DAO–benzoate complex but is increased to 3.3 Å in the complex with imino tryptophan. Todone et al. (1997) suggested that upon reduction the flavin N5 atom most likely becomes protonated, causing the H-bond with the Ala49 backbone N atom to be weakened or even lost in the reduced enzyme.

Even when human DAO is in the oxidized state, the shift in the hydrophobic stretch is more apparent than that seen in the reduced porcine enzyme and raises the question as to how the conformation of the stretch affects the kinetic scheme of the reaction catalyzed by human DAO. Our kinetic data indicate that the rate of flavin reduction is slower in the human enzyme (180 ± 20 sec^{-1}) than in the porcine enzyme (4000 sec^{-1} [Molla et al. 2006]; 1225 sec^{-1} [Pollegioni et al. 1994]), presumably reflecting the different conformations of the hydrophobic stretch. But further analysis of the structure of human DAO in the reduced state will be necessary to fully understand the effect of the stretch conformation on the enzyme's kinetics.

In summary, three-dimensional structural analysis of human DAO revealed that a SAP located at the *si*-face of the flavin ring exists in a significantly different conformation than in porcine DAO. The context-dependent difference in the conformation of the hydrophobic stretch is thought to be a key determinant of the enzyme's affinity for FAD as well as the rate of flavin reduction, thus highlighting the unique features of human DAO. Although purification and crystallization of human DAO is a very difficult task (in large part because of its low affinity for FAD), we are currently working on determining the structure of human DAO in the reduced state. In the present study, we provide the first structural evidence to explain the kinetic difference between the human and porcine enzymes, hopefully facilitating the understanding of this enigmatic enzyme, which may be pivotal for the treatment of disorders related to NMDA dysfunction, such as schizophrenia.

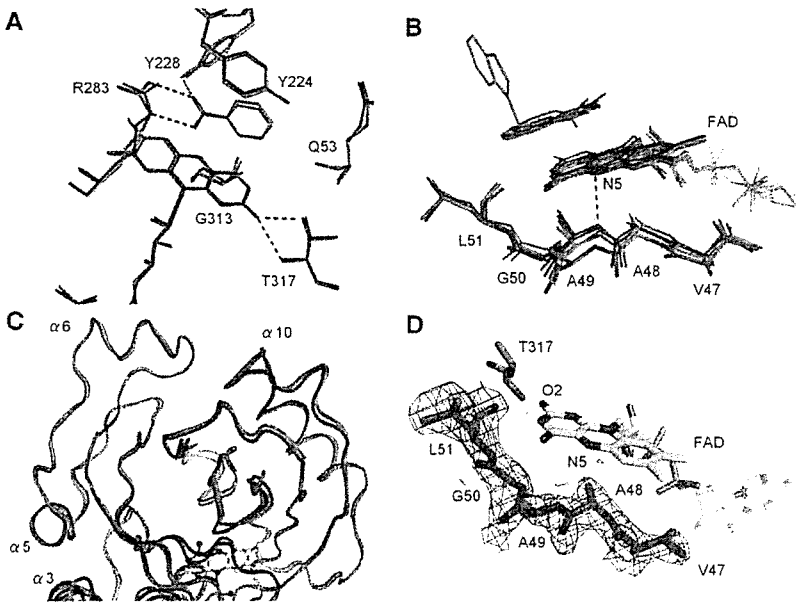

Figure 5. Context-dependent conformational variability of the hydrophobic stretch. *(A)* At the *re*-face of the flavin ring, the active sites are conserved between the human (carbons in green) and porcine (carbons in magenta; PDB code 1VE9) enzymes. H-bonds are shown as dashed lines. *(B)* Context-dependent conformational variability of the hydrophobic stretch (residues 47–51) at the *si*-face of the flavin ring. The hydrophobic stretches of human (carbons in green) and porcine (carbons in magenta; PDB codes 1KIF, 1VE9) DAO showed differing conformations, despite strict sequence identity. The purple intermediate of porcine DAO or the structure in complex with imino tryptophan are also superimposed (carbons in cyan). For clarity, only the H-bond between the flavin N5 atom and the Ala49 backbone N atom in the porcine enzyme (PDB code 1KIF) is shown (dashed line). *(C)* The conformational difference of the hydrophobic stretch (colored in blue) is evident compared with the overall structural similarity between the human (green) and porcine (magenta) DAO structures. *(D)* The hydrophobic stretch of human DAO is shown with an F_o–F_c omit map contoured at 1.0 σ.

Protein Data Bank accession codes

The atomic coordinates and structure factors (code 2DU8) have been deposited in the Protein Data Bank, Research Collaboratory for Structural Bioinformatics, Rutgers University, New Brunswick, NJ (http://www.rcsb.org/).

Materials and methods

Subcloning

The cDNA encoding human kidney DAO (Momoi et al. 1988) was amplified using the N-terminal primer 5′-TCCGGCTG-CTCATATGCGTGTGGTGGTGA-3′ and the C-terminal primer 5′-GCAGCAGTCACATATGTCTTCAGAGGTGG-3′. The PCR product was digested with NdeI and ligated into the similarly restricted pET-11b *E. coli* T7 expression vector (Novagen). The ligated product was introduced into *E. coli* nonexpression host DH5α supercompetent cells. The resultant construct was confirmed by DNA sequencing.

Production

The construct was introduced into an *E. coli* BL21(DE3) strain, after which a single colony of transformants was grown in cultures and stored in 50% (v/v) glycerol at −80°C. Transformants were cultured in terrific broth (1.2% tryptone, 2.4% yeast extract, and 0.4% [v/v] glycerol) with 0.5% (w/v) glucose and 50 mg/L ampicillin at 37°C to an optical density of 0.6 at 600 nm, and then induced with 0.1 mM IPTG. After an additional 24 h, the cells were harvested by centrifugation at 4°C. Usually 30 g of wet cell pellet were obtained from 4 L of culture and were kept frozen at −80°C until used.

Western blotting

Equal amounts of total cellular protein were fractionated on a 12.5% polyacrylamide gel and then transferred to a nitrocellulose membrane (Millipore) at room temperature. DAO was visualized using an ECL detection system (Amersham Biosciences) after incubation with rabbit polyclonal anti-pig kidney DAO primary antibody and a horseradish peroxidase-conjugated donkey anti-rabbit IgG secondary antibody (Promega KK).

Purification

The recombinant human DAO was purified using a modification of the procedure used to purify recombinant porcine DAO (Setoyama et al. 1996). The bacterial pellet was suspended (10 mL/g cell) in 17 mM Na pyrophosphate (pH 8.3) buffer containing 100 μM FAD, 1 mM Na benzoate, 0.3 mM EDTA, 0.5 mM DTT, and 4.5 μg/mL PMSF, after which the cells were disrupted by treatment with 1 mg/mL lysozyme for 1 h, followed by sonication for 30 sec, four times. The disrupted cells were treated with 1% (w/v) streptomycin sulfate, after which the cell debris was removed by centrifugation, and the soluble fraction